Journal of Volcanology and Geothermal Research 310 (2016) 98–106

Contents lists available at ScienceDirect

Journal of Volcanology and Geothermal Research

journal homepage: www.elsevier.com/locate/jvolgeores

Paleoproterozoic felsic volcanism of the Tapajós Mineral Province, Southern Amazon Craton, Brazil

M. Roverato [a,*], D. Giordano [b], C.M. Echeverri-Misas [a], C. Juliani [a]

[a] Universidade de São Paulo, IGC Instituto de Geociências, Departamento de Geologia Sedimentar e Ambiental. Rua do Lago, 562 Cidade Universitária 05508080 - São Paulo, SP-, Brazil
[b] Dipartimento di Scienze della Terra, Università degli Studi di Torino, Via Valperga Caluso, 35, 10125 Torino, Italy

ARTICLE INFO

Article history:
Received 7 May 2015
Accepted 23 November 2015
Available online 4 December 2015

Keywords:
Paleproterozoic volcanism
Felsic ignimbrites
Rheomorphism
Amazon Craton

ABSTRACT

Amazonian rocks record one amongst the most complete and best-preserved Paleoproterozoic magmatic episodes on Earth. The present contribution documents the extremely well preserved paleoproterozoic architecture of a series of felsic rocks found in the Tapajós Mineral Province (TMP), located in the western part of Pará State, southern Amazon Craton, north of Brazil. These rocks are the first to be investigated to comprehend, based on their textural evidences, their emplacement mechanisms. Textural characterization allowed to identify three main facies with, as following reported, 1) chaotic ("Breccia") group, 2) eutaxitic ("Eutax") group and 3) parataxitic ("Paratax") group vitrophyric textures. Given the superb preservation of our samples, the investigated rocks are grouped, according to their grade of welding, into a wide variety of lithofacies from very low-grade to high-grade and rheomorphic ignimbrites. In the "Paratax group" strong similarities with banding in lava flows are observed. Based on the presented data we discuss the effusive or explosive origin of the observed flow mechanisms.

1. Introduction

The study area is located in the southwestern part of the Pará State, north of Brazil and is known as the Tapajós Mineral Province (TMP). The southern part of the TMP (Fig. 1) is poorly known and difficult to access mainly due to the dense forest cover. Besides the geological mapping (at 1:100,000 scale) performed by the Brazilian Geological Survey (CPRM), no detailed fieldwork has been carried out to date. Our field campaign found that granitoid felsic bodies are the prevailing lithotypes, although several volcanic felsic lava flows and volcaniclastic deposits are present. The observed features are consistent with those observed in various other regions in the Amazon Craton also characterized by an ancient volcanism of intermediate to felsic in composition. Rhyolitic lavas, ignimbrites of different welding and rheomorphic grade and rhyolitic breccias are reported by previous authors (Lamarão et al., 2002; Juliani et al., 2005; Lamarão et al., 2005; Juliani and Fernandes, 2010; Fernandes et al., 2011; Vasquez and Dreher, 2011; Silva Simões et al., 2014). The present study is motivated by the fact that many of the silicic volcanic products have been interpreted either as lava flows or as densely welded/rheomorphic ignimbrites. Due to the occurrence of the process of rheomorphism and welding of volcanic materials that could potentially obliterate the original deposit structure and sample texture, distinguishing the fragmental or coherent nature of certain deposits, felsic or not, is sometime controversial and requires a careful investigation (e.g. Branney et al., 1992; Smith and Cole, 1997; Pioli and Rosi, 2005; Quane et al., 2009; Andrews and Branney, 2011). Ancient volcanic regions represent a challenge for the understanding of emplacement dynamics especially when the stratigraphic relationships of the deposits are difficult to decipher or blurred by erosion or vegetation cover. We aim here to improve the current knowledge of felsic volcanics investigated in the Amazon Craton by adding new textural and petrographic data useful to better constrain this still poorly known rhyolitic volcanism. This contribution aims to shed light into some of the volcanic processes that occurred in the TMP in order to better constrain the geological features of the Amazon Craton.

2. Geological and tectonic setting

The Amazonian Craton (Almeida et al., 1981) is one of the largest Precambrian terrains in the world, occupying approximately half of the Brazilian territory. It is a large Archean platform reworked and reactivated during the ca. 2100 Ma Trans-Amazonian event (Amaral, 1974; Hasui et al., 1993; Costa and Hasui, 1997). All volcanic/plutonic rocks forming the craton are attributed to the Uatumã Supergroup that extends to an area larger than 1,200,000 km^2. These rocks were attributed, by previous authors, to a single magmatic pulse generated by a large scale extensional event of the Amazonian Craton (Santos, 1984). However, according to Dall'Agnol et al. (1994, 1999) and Lamarão et al. (1999) this supergroup is heterogeneous and includes

* Corresponding author.

http://dx.doi.org/10.1016/j.jvolgeores.2015.11.019
0377-0273/

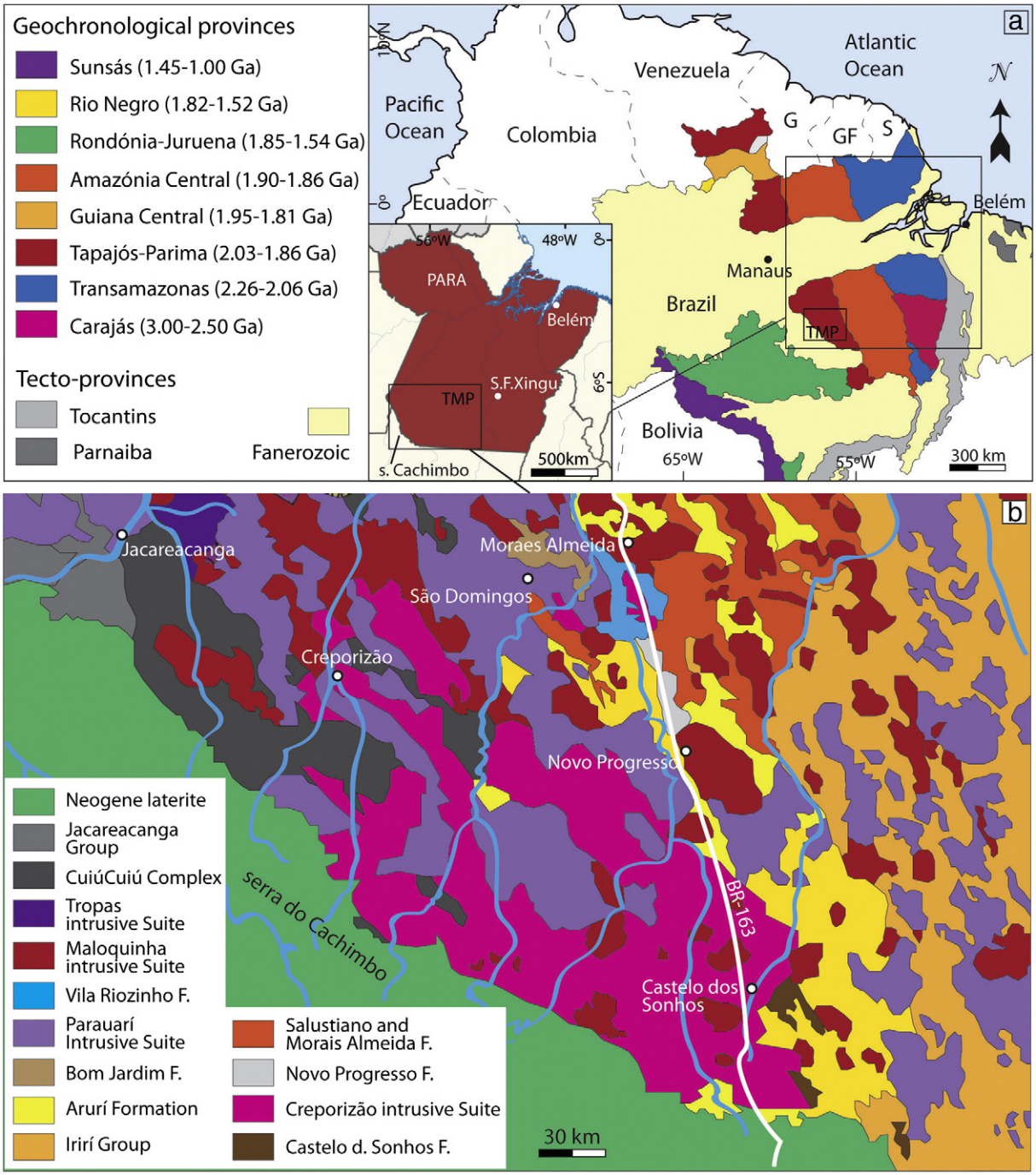

Fig. 1. (a) Location map of the Amazonian Craton divided in eight geochronological/tectonic provinces in accordance with Santos (2003); G = Guyana, GF = French Guyana, S = Suriname. (b) Geological map of the southern Tapajós Mineral Province (simplified from Juliani et al., 2014); TMP = Tapajós Mineral Province.

Table 1
Major element composition of collected samples.

Sample	39B	79	84A	101	156B	173	176	178B	179	180	183A	184	C0-67
SiO_2	65.32	71.8	68.15	72.22	71.59	75.58	75.93	70.86	72.53	69.73	71.25	70.99	70.81
TiO_2	0.86	0.34	0.48	0.32	0.36	0.2	0.2	0.39	0.37	0.44	0.41	0.37	0.40
Al_2O_4	16.62	14.17	15.44	14.29	14.28	12.97	12.72	14.63	14.45	15.3	14.66	14.55	14.77
Fe_2O_3	3.63	1.57	2.25	1.49	1.54	1.1	0.87	1.74	1.86	2.26	1.74	1.94	1.7
MnO	0.09	0.04	0.09	0.04	0.04	0.07	0.06	0.07	0.09	0.09	0.09	0.08	0.09
MgO	0.51	0.32	0.54	0.25	0.19	0.19	0.16	0.29	0.3	0.36	0.24	0.3	0.35
CaO	2.07	1.04	0.98	0.59	0.5	0.72	0.34	0.88	0.65	0.88	0.56	0.68	0.91
Na_2O	4.99	3.75	4.56	4.12	3.63	3.21	3.46	4.7	4.38	4.49	4.54	4.97	4.42
K_2O	3.88	5.73	5.63	5.6	5.6	5.18	5.11	5.11	5.56	5.64	5.57	4.87	5.71
P_2O_5	0.22	0.04	0.09	0.04	0.04	0.02	0.01	0.06	0.06	0.07	0.05	0.06	0.07
LOI	1.5	0.99	1.34	0.82	1.28	1.49	0.88	1.28	0.85	1.0	0.81	1.07	1.03
Total	99.87	99.88	99.82	99.94	99.19	100.78	99.79	100.22	101.19	100.28	100.01	100.16	100.51

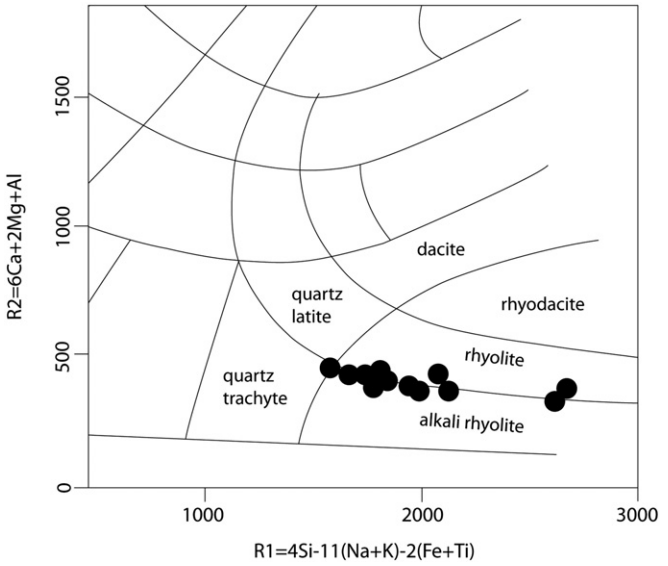

Fig. 2. Classification diagram R1 vs. R2 (De La Roche et al., 1980) for the studied rock samples.

not only one but several volcanic units. Based on geochronological data, Cordani and Brito Neves (1982), Teixeira et al. (1989), Tassinari and Macambira (1999) and Santos et al. (2000), divided the craton into several, predominantly NW-oriented, provinces, which have been interpreted as successive continental accretionary events, granitic magmatism and tectonic reworking. Following the ideas of Tassinari and Macambira (1999), the craton can be divided into six geochronological provinces, whereas Vasquez et al. (2008), based on Santos (2003), proposed to divide the craton in eight geochronological provinces (Fig. 1a). TMP is situated mostly in the Tapajós–Parima (Santos et al., 2000) geochronological/tectonic province with the eastern part belonging to the Amazonia Central geochronological/tectonic province (Fig. 1a). Based on Sm–Nd data and U–Pb ages (2.1–1.87 Ga), Santos et al. (2001, 2004) and Vasquez et al. (2008), identified several different domains for the Tapajós–Parima geochronological province and consider the TMP as constituted by a sequence of continental magmatic arcs (Cuiú-Cuiú (ca. 2.01 G), Jamanxim, Creporizão (1.98–1.97 Ga), Tropas (ca. 1.9 Ga) and Parauari (ca. 1.9–1.88 Ga) followed by the Maloquinha anorogenic alkaline magmatism (Santos et al., 2000, 2001, 2004) (Fig. 1b). These units are progressively younger from southwest toward northeast pointing to a subduction zone in the Serra do Cachimbo Graben region and a continental zone in the São Félix do Xingu area within a *flat-subduction* scenario with continental arc migration from the Tapajós province to the Xingu region (Juliani et al., 2009).

2.1. Paleoproterozoic volcanism of the TMP

Late Paleoproterozoic volcanism of the Tapajós domain represented by the Iriri group (Fig. 1b) is divided in Salustiano and Aruri formations consisting of rhyolites, dacites and their pyroclastic and epiclastic derivatives (Pessoa et al., 1977) and Bom Jardim formation (Almeida et al., 2000). The latter formation is characterized by mafic to intermediate

Fig. 3. Photographs of four outcrops showing the transition between (a) slightly welded, (b) moderate-grade welded, (c) rheomorphic and (d) lava-like felsic bodies. Pictures (a and b) clearly show the particulate nature of the deposit while the clastic character of the outcrop in the picture (c) is slightly visible blurred by the rheomorphic process. Picture (d) displays strong lineations and convolute folds, features shared both by high-grade rheomorphic ignimbrites and banded-lavas that make their difficult discrimination.

high-K to shoshonitic calc-alkaline rocks (1898 ± 5 Ma, Santos et al., 2001). Juliani et al. (2005) considered the Bom Jardim volcanism as a preliminary step of the Iriri event representing pre-caldera volcanism followed by the Salustiano and Aruri caldera-related felsic activity. Intense hydrothermal alteration induced by epithermal high-sulfidation *Au*-mineralization characterizes the area (Juliani et al., 2005). Post-caldera volcanism is characterized by ring-felsic volcanic structures that produced A-type alkaline (Vasquez and Dreher, 2011) rhyolitic lavas and volcaniclastic flows. Lamarão et al. (2002, 2005) also described the felsic A-type alkaline volcanism (named as Moraes Almeida volcanic sequence) represented by lavas and ignimbrites as part of the Iriri group. They described the latter products as "reddish brown, strongly welded and oxidized, rich in crystals fragments and mm- to cm-sized lithic fragments" (Lamarão et al., 2002) without an in depth textural analysis of the rocks. These authors dated zircons of the investigated rocks and found ages in the interval between 1875 ± 4 and 1890 ± 6 Ma. Further investigation on the felsic A-type volcanism of the Iriri group from Juliani et al. (2014) also establishes a relationship between this and the Santa Rosa Formation (1.87 Ga) in the Xingu region. This formation is characterized by felsic A-type alkaline volcanism which is considered to be related to a fissure-fed evolutionary model and caldera-related systems (Juliani and Fernandes, 2010; Fernandes et al., 2011).

3. Compositional and petrological analysis

Whole rock analyses (Table 1) exhibit mainly alkali–rhyolite to rhyolite compositions with SiO_2 content ranging from 65 to 76 wt.% and an alkali content of 9–10 wt.% with an average K_2O/Na_2O ratio of 1.23 (Fig. 2). Our samples display an original crystal content ranging from ca. 5 to 45 vol.%, a minor lithic clast population constituted of lavas and devitrified fragments immersed in a fine groundmass composed of quartz, potassic feldspar, cloritized biotite and sericite. The phenocryst assemblage consists of plagioclase, potassic feldspar and a small amount of Fe–Mg-phases and quartz. Plagioclase crystals range from subhedral to anhedral, are commonly fragmented and show moderate to intense resorption and sieve texture indicating non-equilibrium conditions during magma transport. A few of them show distortion probably developed during flow and jigsaw-fit fractures. Potassic feldspar

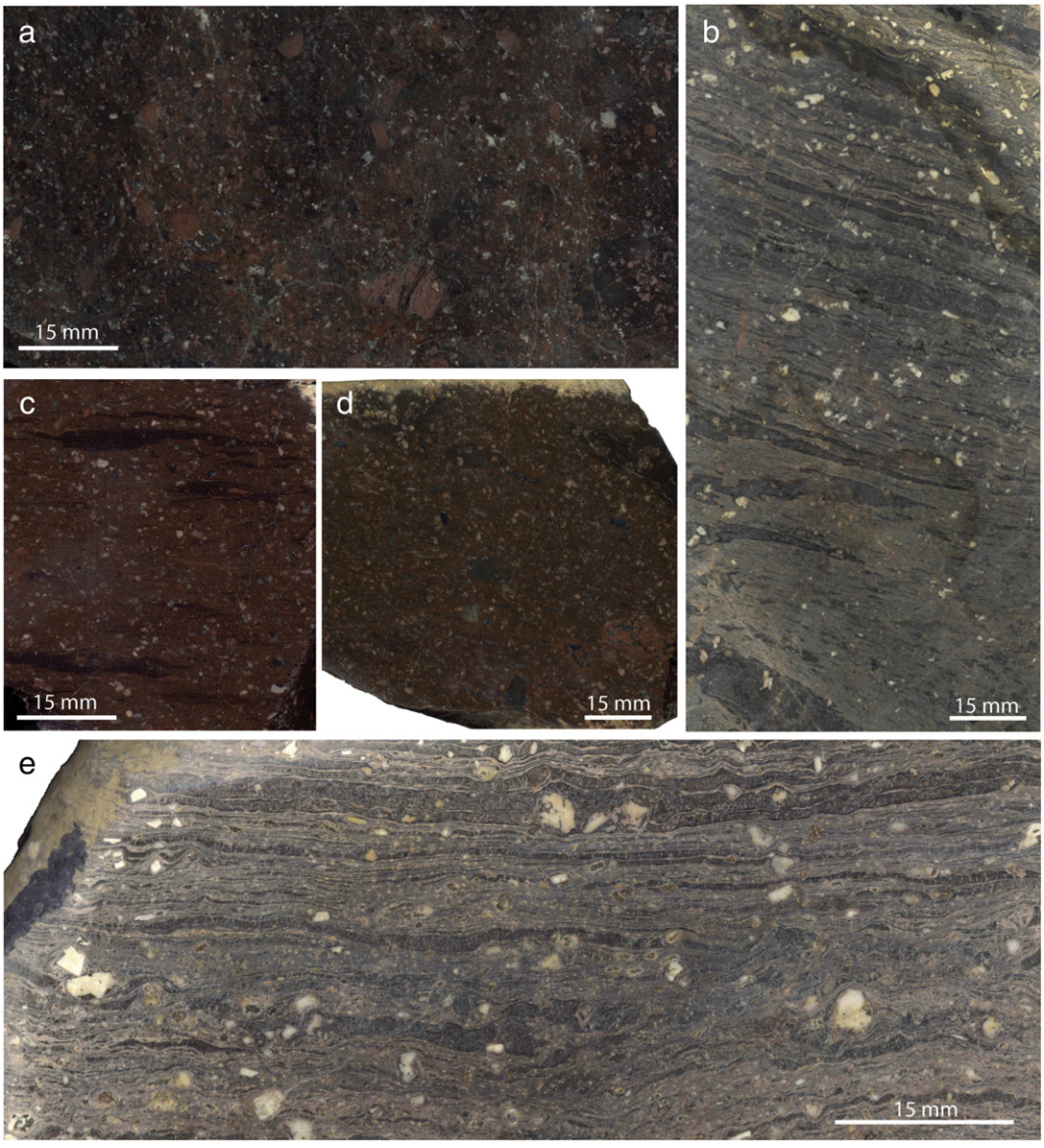

Fig. 4. Scanned images of the polished hand-scale samples collected in the field showing the different grades of welding. Picture (a) shows a rhyolitic ignimbritic breccia, (b, c and d) display different grades of the eutaxitic fabric, (e and f) show the parataxitic texture.

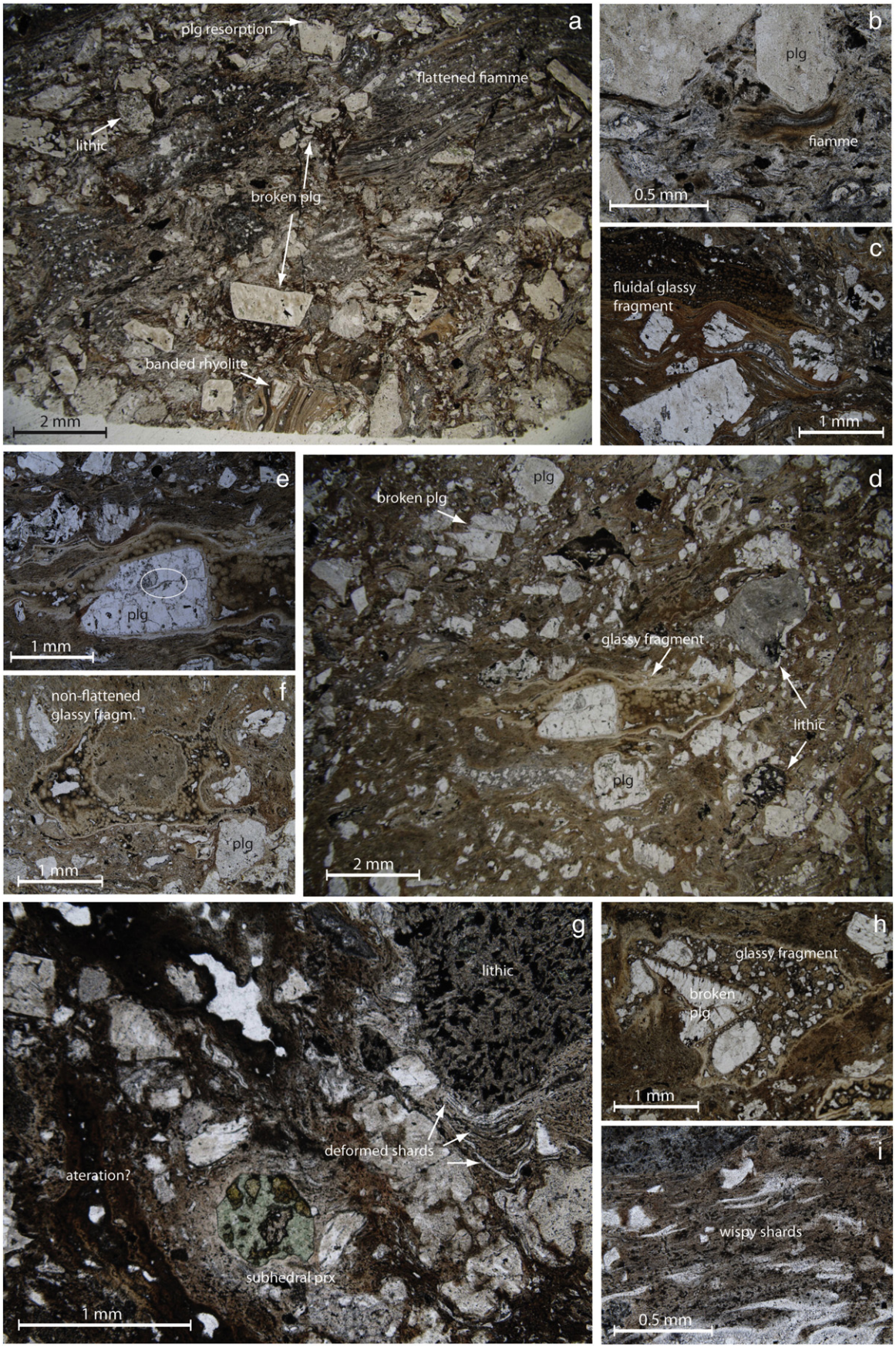
a
plg resorption
flattened fiamme
lithic
broken plg
banded rhyolite
2 mm
b
plg
fiamme
0.5 mm
c
fluidal glassy fragment
1 mm
d
plg
broken plg
glassy fragment
lithic
plg
2 mm
e
plg
1 mm
f
non-flattened glassy fragm.
plg
1 mm
g
lithic
deformed shards
ateration?
subhedral prx
1 mm
h
glassy fragment
broken plg
1 mm
i
wispy shards
0.5 mm

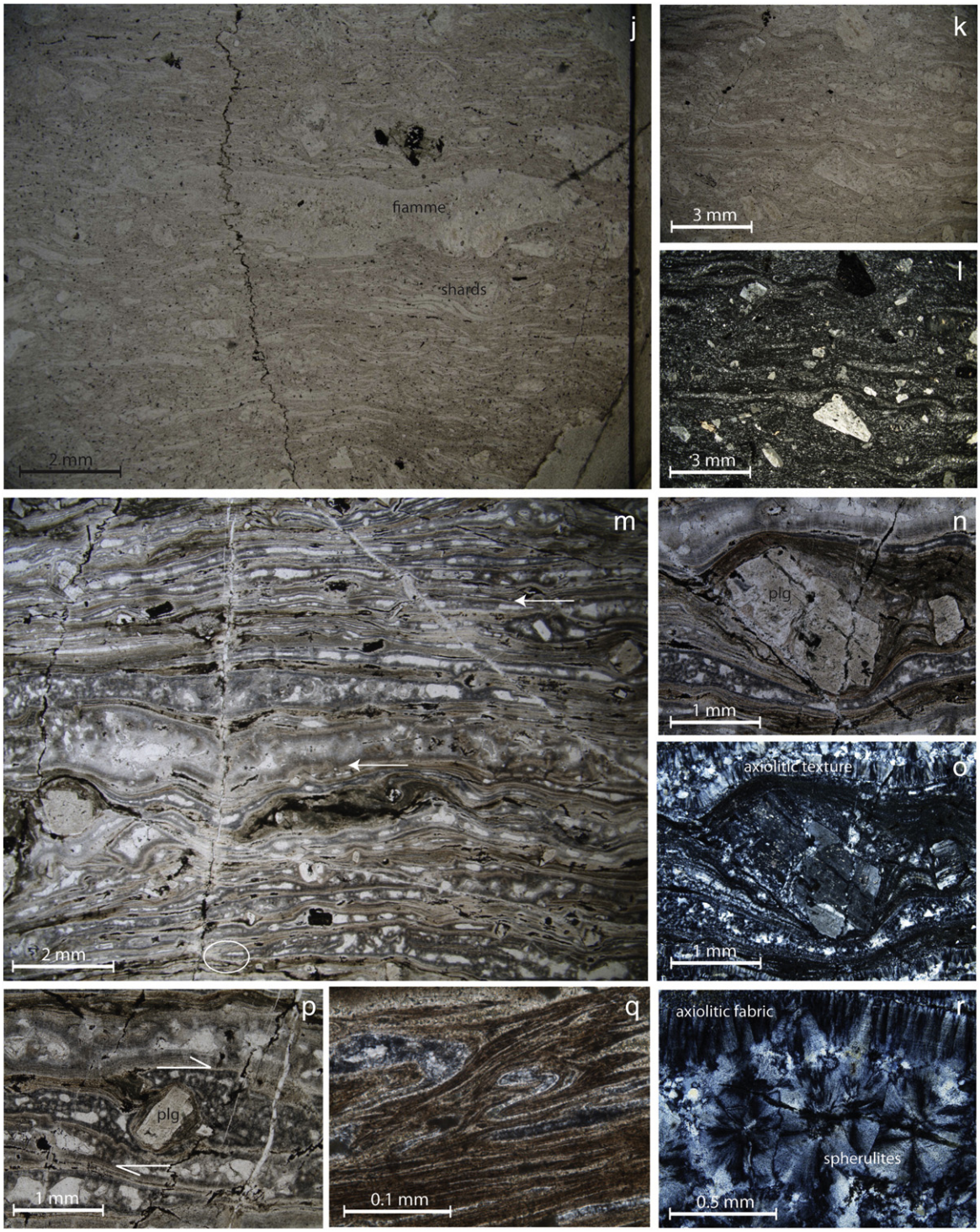

Fig. 5. Photomicrographs showing the different textures present in the collected samples. (a and d) "Panoramic" images of the "Breccia group" showing the population of lithics, banded-rhyolite fragments, ehuedral/subhedral and broken plagioclase crystals, "glassy" deformed and (c) fluidal fragments immersed in a microcrystalline matrix. (a and b) Some flattened fiammes display a thin parallel layering that represent the compaction of pumice vesicle-walls. (e and h) Compacted and stretched devitrified fragment displaying spherulites and a broken plg crystal that shows displacement and pull-apart structure (e — white circle). (f) Some "glassy" clasts present non-flattened. (g and i) Other characteristic of compaction of hot pyroclasts is the presence of micrometer shards stretched and deformed around lithics and crystals. The subhedral pyroxene in figure (g) displays a chlorite (green aspect) and titan (light-brown stains) that substitute the original composition of the crystal. The eutaxitic fabric in well represented by the microphotographs (j), (k) and (l). The flattened fiammes and shards organize in sub-parallel bedding and deform around crystals due to the compaction of hot low-viscous pyroclasts. (l) X-nicols image evidences the "pepper–salt" microcrystalline matrix formed mainly by K-fld and quartz. (m) "Panoramic" image of the parataxitic fabric showing continuum bedding of "glassy" streaks deformed around crystals (n and o). Some indicators can suggest the flowing direction such as imbricated (m — top-right arrow, n, o) and rotated crystals (m — central arrow, p). Some streaks present abrupt termination as indicated in figure (m) (white circle) that could be an indicator of the particulate nature of the deposit. Figure (q) shows micrometric folds related to ductile shearing. (o and r) X-nicols images showing the devitrified character of the deposits represented by spherulites and axiolitic texture.

crystals are anhedral and present mainly in the matrix associated with sericite. Rare phenocrysts of quartz present bipyramidal habit or display rounded edges due to the reabsorption processes with a matrix. The microcriystallinity of the groundmass (visible in cross-polarized light), which we define as "pepper–salt", is a micro-granophiric-like devitrification texture characterized by crystallization of amorphous quartz (cristobalite) and alkali feldspar. Samples are generally affected by variable intensity of hydrothermal alteration. Plagioclase phenocrysts present diffuse potassic and less propylictic alterations. Groundmass is affected by sericitic alteration.

4. Ignimbritic textures: A review

Explosively generated fragmental deposits may weld, under certain conditions, and start to flow viscously (e.g. Heap et al., 2014; Kolzenburg and Russell, 2014; Wadsworth et al., 2014). Manley (1996) suggested that vitric fragments such as shards and pumices begin to distort and stretch up to the volcaniclastic flow becomes completely layered/banded in a viscous manner (Andrews and Branney, 2011; Castro et al., 2014). Since the discovery of welded ignimbrites during 1960s (Smith, 1960; Ross and Smith, 1961; Schmincke and Swanson, 1967; Walker and Swanson, 1968) there has been lot of controversy related to recognition, origin, transport and emplacement mechanisms of intensely welded to rheomorphic ignimbrites. The absence of unequivocal vitroclastic textures complicates the distinction between volcaniclastic and layered lava flows. Walker (1983) introduced the concept of "grade of welding" that refers to the amount of welding and compaction exhibited by ignimbrites. A wide variety of ignimbrite lithofacies ranging from very low-grade slightly welded to very high-grade "lava-like", through intensely welded to rheomorphic. Andrews and Branney (2011) highlight that welding and rheomorphism are favored by low-viscosity pyroclasts (Quane and Russell, 2005; Russell and Quane, 2005) that are strongly promoted by high emplacement temperature (Russell et al., 2003), strongly peralkaline composition (Wolff and Wright, 1981; Dingwell and Romano, 1998), porosity and dissolved water (Guest and Rogers, 1967; Bierwirth, 1982; Grunder et al., 2005; Grunder and Russell, 2005; Robert et al., 2008; Heap et al., 2014; Kolzenburg and Russell, 2014). An emplacement condition that minimizes cooling of the magma such as voluminous eruptions (Bachmann et al., 2000) with low pyroclastic fountaining (e.g., minimal air ingestion and cooling) also favors low viscosities. Several authors suggested that welding and rheomorphism occur as flow and post-depositional processes. Ragan and Sheridan (1972) found that the rotated lithic clasts and rotated segments of broken fiamme might be the results of post emplacement loading. Wolff and Wright (1981) further proposed that lineation of high-grade ignimbrites is diagnostic of post-depositional "re-flowing" in contrast to the idea of Chapin and Lowell (1979) and Reedman et al. (1987) that consider these features as formed during initial deposition. Moreover, the idea that welding and rheomorphism are not always a mere post-depositional processes has been recently supported by different authors that provided evidence that welding of pyroclasts occurs syn-depositionally within the flow due to the sticking of, commonly, low viscosity particles (Branney and Kokelaar, 1992; Branney et al., 1992; Smith and Cole, 1997; Pioli and Rosi, 2005; Andrews et al., 2008). Rheomorphism, such as banding in lavas, can be, in fact, characterized by ductile folds generated during and independently of the main flow. In the case of ignimbrites these features are associated with prolate, elongated fiamme and vesicles (Schmincke and Swanson, 1967; Chapin and Lowell, 1979; Wolff and Wright, 1981; Branney et al., 1992; Sumner and Branney, 2002; Pioli and Rosi, 2005; Andrews and Branney, 2011; Brown and Bell, 2013). When the coalescence of "soft" pyroclasts reaches very high grades and the rheomorphism develops deeply in the ignimbrite the original clast features are totally obliterated and the deposit appears as a flow-banded lava-like (Andrews and Branney, 2011) that complicate the discrimination with a lava flow.

5. Textural analyses

In the following section we present the volcanic rocks (Fig. 3) studied in the field close to the Novo Progresso and Castelo dos sonhos villages (Fig. 1b). Details of macroscopic and microscopic textures of our samples are given in Figs. 4 and 5, respectively. We divided macroscopically our samples in three main textural groups that display chaotic ("Breccia") group (Fig. 4a), eutaxitic ("Eutax") group (Fig. 4b, c, d) and parataxitic ("Paratax") group (Fig. 4e) vitrophyric textures as described below.

5.1. The Breccia group

The Breccia group is characterized by matrix-supported texture with sub-rounded to angular clasts and deformed fragments of different lithologies. Lithologies vary from reddish and dark massive lava lithics, to welded-tuff lithics, banded rhyolite fragments, ehuedral, subhedral and broken crystals, shards and scattered low to medium/high deformed devitrified fiamme (Figs. 4a and 5a–g). Several, and often all, of these lithotypes can be found in a single rock sample of the Breccia group.

5.2. The Eutax group

The Eutax group shows moderately to strongly flattened glassy fragments (fiamme) that form discontinuous and non-homogeneous layering. Eutaxitic texture is shown in Fig.4b/c/d. Fig. 4c displays well-stretched fiamme, varying from millimetric to 3–4 cm in size, immersed in a homogeneous reddish matrix; no lithics are present. The sample in Fig. 4d is polylithologic in composition. Fiamme and lithics as well as glassy fragments slightly- to well-stretched are observed in this rock. The microphotographs of the Eutax group in Fig. 5h/i/j/k/l show the eutaxitic fabric with viscously deformed fiamme and shards immersed in a microcrystalline matrix. Note that sample represented in Fig. 4b shows both eutaxitic and parataxitic fabric. Wispy shard-like fragments are present (Fig. 5i) and are found in pressure shadows adjacent to crystals or lithics. Fiamme, shards and glass matrix are completely devitrified. Feldspar crystallites form distinct bundles, many of which display spherulitic growth (Fig. 5r) around a central nucleus of feldspar, whereas others display axiolitic growth characterized by crystals radiating from the walls toward the inner part of the glassy fragments (Fig. 5r).

5.3. The Paratax group

The Paratax group (Fig. 4e) comprises elongate, thin, dark and light bands and boudinaged fiamme. The original vitrous fragments are in most cases approaching homogenization; Fig. 4e shows some clastic glassy fragments whit abrupt terminations. Parataxitic fabric typically displays subhorizontal bands (Fig. 5m), although, in places, intricate small-scale intrafolial folds are present (Fig. 5q). The bands are deformed and flattened around lithic fragments and crystals (Fig. 5n/o/p), some of them being rotated (Fig. 5p). All the vitrofiric components of this group are completely devitrified and display features described above for the Eutax group.

6. Discussion and conclusive remarks

The detailed description and classification of textural features allow us to distinguish between different transport and emplacement mechanisms associated to effusive and explosive eruptive styles. Under certain conditions (i.e. intense welding or rheomorphism) the differences between the flow mechanisms are frequently not clearly distinguishable;

being particularly complex in strongly altered or poorly exposed volcanic successions as those described above. This work allowed us to establish, based on variations in textural facies, the distinction of three main typologies of felsic volcanic rocks. The Breccia group is characterized by the presence of material of fragmental origin. Vitric fragments (although devitrified and altered), lithics and broken crystals suggest the explosive nature of these deposits. Juvenile fragments are deformed around lithic clasts and crystals or compacted in the matrix implying welding likely promoted by hot sedimentation. Some of our specimens display both deformed *fiamme* with wispy or ragged terminations and discontinuous streaks that may be related to different grades of agglutination (dynamic process requiring transport) of hot fragments. The variation in welding characters and gradation of eutaxitic/parataxitic flow-laminated (reomorphic) tuffs from the more particulate flow deposits strongly suggest that the rhyolites are pyroclastic in origin. Strongly layered and folded rocks with no univocal clastic character are the most complex to interpret, as a clear distinction between lavas and particulate flows (Figs. 3d and 4e) was not possible. Eruption dynamic associated to middle- to high-grade rheomorphism of silicic volcanics and rhyolitic-banded lava flows is both favored by low viscosity high temperature condition emplacement. This promotes the high flow-mobility and could explain the presence of silicic large volcanic areas characteristic of the ancient Amazonian volcanism. The Uatumã Supergroup, both plutonic and extrusive magmatism, has an extension of more than 1,200,000 km^2 constituted in part by volcanic deposits ranging from andesitic to rhyolitic in composition. The real extension of the felsic volcanism is still poorly known as well as its origin. Previous authors mentioned that the felsic products present in the Amazon Craton could be related to caldera-type systems (Lamarão et al., 2002; Juliani et al., 2005; Lamarão et al., 2005; Pierosan et al., 2011). Later, Juliani and Fernandes (2010), inspired by the model of Aguirre-Diaz and Labarthe-Hernandez (2003), suggested a fissure-fed evolutionary model for the felsic Santa Rosa Formation in the Xingu region. The model for fissure ignimbrites used by Aguirre-Diaz and Labarthe-Hernandez (2003) to explain the "Sierra Madre Occidental" formation is similar to those proposed for calderas; "the main differences are the batholithic size of the magma chamber(s) to account for the impressively large volume of the ignimbrite package of the Sierra Madre Occidental and the fissure-type vent and/or vents aligned along a normal fault instead of forming an arcuate structure". We still cannot fully support any specific model due to the lack of strong data. Nonetheless, inspired by the work of Juliani and Fernandes (2010), we propose that a fissure-fed volcanism, similar to that proposed by these authors for the nearby Xingu region, could be used to explain the features of the TMP volcanic rocks object of the present contribution. Although a more detailed field campaign and detailed mapping of the area will be necessary in order to reconstruct the previous volcanic landscapes (e.g. paleo-vents, feeding-systems) and their distribution. Additional textural studies will have to be carried out to describe more in depth flow features of volcanic structures and samples.

Acknowledgments

This work was supported by the project CAPES/CNPq 402564/2012-0 (Programa Ciências sem Fronteiras) to Caetano Juliani and Matteo Roverato. M. Roverato acknowledges the grant of the Brasilian CAPES/CNPq Programa Ciências Sem Fronteiras, Atração de Jovem Talento 402564/2012-0. We acknowledge the CNPq/CT-Mineral (Proc. 550.342/2011-7) and the INCT-Geociam (573733/2008-2) — (CNPq/MCT/FAPESPA/PETROBRAS). D. Giordano acknowledges the financial support for this research from the CAPES project (proposal 302827) of the Ciências Sem Fronteiras program (Brazil) and the local research funds (2012, 2013, 2014) of the University of Turin (Ex60-2012 (D15E12002650005)). We would like to acknowledge Stephan Kolzenburg for the thoughtful comments and suggestions and Joan Marti and an anonymous reviewer for improving the manuscript.

References

Aguirre-Diaz, G.J., Labarthe-Hernandez, G., 2003. Fissure ignimbrites: fissure-source origin for voluminous ignimbrites of the Sierra Madre Occidental and its relationship with Basin and Range faulting. Geology 31, 773–776.
Almeida, F.F.M., Hasui, Y., Brito Neves, B.B., Fuck, R.A., 1981. Brazilian structural provinces: an introduction. Earth Sci. Rev. 17, 1–29.
Almeida, M.E., Brito, M.F.L., Ferreira, A.L., Monteiro, M.A.S., 2000. Projeto Especial Província Mineral do Tapajós. Geologia e recursos minerais da Folha Vila Mamãe Anã (SB.21-V-D). Estados do Pará e Amazonas. CPRM, Brasília.
Amaral, G., 1974. Geologia Pré-Cambriana da Região Amazônica. Tese de Livre Docência, IG/USP (212 pp.).
Andrews, G.D.M., Branney, M.J., 2011. Emplacement and rheomorphic deformation of a large, lava-like rhyolitic ignimbrite: Grey's Landing, southern Idaho. Geol. Soc. Am. Bull. 123, 725–743.
Andrews, G.D.M., Branney, M.J., Bonnichsen, B., McCurry, M., 2008. Rhyolitic ignimbrites in the Rogerson Graben, southern Snake River Plain volcanic province: volcanic stratigraphy, eruption history and basin evolution. Bull. Volcanol. 70, 269–291.
Bachmann, O., Dungan, M.A., Lipman, P.W., 2000. Voluminous lava-like precursor to a major ash-flow tuff: low-column pyroclastic eruption of the Pagosa Peak Dacite, San Juan volcanic field, Colorado. J. Volcanol. Geotherm. Res. 98, 153–171. http://dx.doi.org/10.1016/S0377-0273(99)00185-7.
Bierwirth, P.N., 1982. Experimental welding of volcanic ash, Unpubl. B.Sc. Hons. Thesis, Monash University.
Branney, M.J., Kokelaar, B.P., 1992. A reappraisal of ignimbrite emplacement: progressive aggradation and changes from particulate to non-particulate flow during emplacement of high-grade ignimbrite. Bull. Volcanol. 54, 504–520.
Branney, M.J., Kokelaar, B.P., McConnell, B.J., 1992. The Bad Step Tuff: a lava-like rheomorphic ignimbrite in a calc-alkaline piecemeal caldera, English Lake District. Bull. Volcanol. 54, 187–199.
Brown, D.J., Bell, B.R., 2013. The emplacement of a large, chemically zoned, rheomorphic, lava-like ignimbrite: the Sgurr of Eigg Pitchstone, NW Scotland. J. Geol. Soc. 170, 753–767. http://dx.doi.org/10.1144/jgs2012-147.
Castro, J., Bindeman, I., Tuffen, H., Schipper, C., 2014. Explosive origin of silicic lava: textural and δD-H_2O evidence for pyroclastic degassing during rhyolite effusion. Earth Planet. Sci. Lett. 405, 52–61.
Chapin, C.E., Lowell, G.R., 1979. Primary and secondary flow structures in ash-flow tuffs of the Gribbles Run paleovalley, central Colorado. Spec. Pap. Geol. Soc. Am. 180, 137–154.
Cordani, U.G., Brito Neves, B.B., 1982. The geological evolution of South America during the Archean and Early Proterozoic. Rev. Bras. Geosci. 12, 78–88.
Costa, J.B.S., Hasui, Y., 1997. Evolução geológica da Amazônia. In: Costa, M.L., Angélica, R.S. (Eds.), Contribuições à geologia da Amazônia, pp. 16–90.
Dall'Agnol, R., Lafon, J.M., Macambira, M.J.B., 1994. Proterozoic anorogenic magmatism in the Central Amazonian Province, Amazonian Craton: geochronological, petrological and geochemical aspects. Mineral. Petrol. 50, 113–138.
Dall'Agnol, R., Costi, H.T., Leite, A.A.S., Magalhaes, M.S., Teixeira, N.P., 1999. Rapakivi granites from Brazil and adjacent areas. Precambrian Res. 95, 9–39.
De La Roche, H., Leterrier, J., Grand Claude, P., Marchal, M., 1980. A classification of volcanic and plutonic rocks using R1R2-diagramandmajor-element analyses — Its relationships with current nomenclature. Chem. Geol. 29, 183–210.
Dingwell, D.B., Romano, K.U.H.C., 1998. Extremely fluid behavior of hydrous peralkaline rhyolites. Earth Planet. Sci. Lett. 158, 31–38.
Fernandes, C.M.D., Juliani, C., Monteiro, L.V.S., Lagler, B., Misas, C.M.E., 2011. High-K calc-alkaline to A-type fissure-controlled volcano-plutonism of the São Félix do Xingu region, Amazonian craton, Brazil: exclusively crustal sources or only mixed Nd model ages? J. S. Am. Earth Sci. 32 (4), 351–368.
Grunder, A., Russell, J.K.R., 2005. Welding processes in volcanology: insights from field, experimental, and modeling studies. J. Volcanol. Geotherm. Res. 142, 1–9.
Grunder, A., Laporte, D., Druitt, T.H., 2005. Experimental and textural investigation of welding: effects of compaction, sintering vapor-phase crystallization in the rhyolitic Rattlesnake Tuff. J. Volcanol. Geotherm. Res. 142, 89–104.
Guest, J.E., Rogers, P.S., 1967. The sintering of glass and its relationship to welding in ignimbrites. Proc. Geol. Soc. Lond. 1641, 174–177.
Hasui, Y., Haraly, N.L.E., Schobbenhaus, C., 1993. Megaestruturação Pré-Cambriana do território brasileiro baseada em dados geofísicos e geológicos. Geociências 12, 7–31.
Heap, M.J., Kolzenburg, S., Russell, J.K., Campbell, M.E., Welles, J., Farquharson, J.I., Ryan, A., 2014. Conditions and timescales for welding block and ash flow deposits. J. Volcanol. Geotherm. Res. 289, 202–209.
Juliani, C., Fernandes, C.M.D., 2010. Well-preserved Late Paleoproterozoic volcanic centers in the São Félix do Xingu region, Amazonian Craton, Brazil. J. Volcanol. Geotherm. Res. 191, 167–179.
Juliani, C., Rye, R.O., Nunes, C.M.D., Snee, L.W., Correa Silva, R.H., Monteiro, L.V.S., Bettencourt, J.S., Neumann, R., Neto, A.A., 2005. Paleoproterozoic high sulphidation mineralization in the Tapajós gold province, Amazonian Craton, Brazil: geology, mineralogy, alunite argon age, and stable-isotope constraints. Chem. Geol. 215, 95–125.
Juliani, C., Fernandes, C.M.D., Monteiro, L.V.S., Misas, C.M.E., Lagler, B., 2009. Possível zonamento metalogenético associado ao evento vulcano-plutônico de ~2,0 a 1,88 Ga na parte sul do Cráton Amazônico. In: UFRGS (Ed.), Simpósio Brasileiro de Metalogenia, 2 ed Gramado ((in Portuguese), CD-ROM).
Juliani, C., Vasquez, M.L., Klein, E.L., Villas, R.N., Echeverri-Misas, C.M., Santiago, E.S.B., Monteiro, L.V.S., Carneiro, C.C., Fernandes, C.M.D., Usero, G., 2014. Metalogenia da Província Tapajós. In: Silva M.G.; Jost H.; Kuyumajian R.M. (Org.). Metalogênese das

Províncias Tectônicas Brasileiras. 1 ed. : CPRM — Serviço Geológico do Brasil, 1, 51–90.
Kolzenburg, S., Russell, J.K., 2014. Welding of pyroclastic conduit infill: a mechanism for cyclical explosive eruptions. J. Geophys. Res. 119, 5305–5323.
Lamarão, C.N., Dall'Agnol, R., Lafon, J.M., Lima, E.F., 1999. As associaç¸es vulcânicas e plutônicas de Vila Riozinho e Morais Almeida, Província Aurífera do Tapajoós, SW do estado do Para'. Simpo' sio sobre Vulcanismo e Ambientes Associados. 1, Gramado*/RS, Boletim de resumos, p. 93 (in Portuguese).
Lamarão, C.N., Dall'Agnol, R., Lafon, J.-M., Lima, E.F., 2002. Geology, geochemistry, and Pb–Pb zircon geochronology of the Paleoproterozoic magmatism of Vila Riozinho, Tapajos Gold Province, Amazonian craton, Brazil. Precambrian Res. 119, 189–223.
Lamarão, C.N., Dall'Agnol, R., Pimentel, M.M., 2005. Nd isotopic composition of Paleoproterozoic volcanic and granitoid rocks of Vila Riozinho: implications for the crustal evolution of the Tapajos gold province, Amazon craton. J. S. Am. Earth Sci. 18, 277–292.
Manley, C.R., 1996. In situ formation of welded tuff-like textures in the carapace of a voluminous silicic lava flow, Owyhee County, SW Idaho. Bull. Volcanol. 57, 672–686. http://dx.doi.org/10.1007/s004450050120.
Pessoa, M.R., Andrade, A.F., Nascimento, J.O., Santos, J.O.S., Oliveira, J.R., Lopes, R.D., Prazeres, W.V., 1977. Projeto Jamanxim. DNPM/CPRM, Manaus (in Portuguese).
Pierosan, R., Lima, E.F., Nardi, L.V.S., Campos, C.P., Bastos Neto, A.C., Ferron, J.M.T.M., Prado, M., 2011. Paleoproterozoic (~1.88 Ga) felsic volcanism of the Iricoumé Group in the Pitinga Mining District area, Amazonian Craton, Brazil: insights in ancient volcanic processes from field and petrologic data. An. Acad. Bras. Cienc. 83 (3), 921–937.
Pioli, L., Rosi, M., 2005. Rheomorphic structures in a high-grade ignimbrite: the Nuraxi tuff, Sulcis volcanic district (SW Sardinia, Italy). J. Volcanol. Geotherm. Res. 142, 11–28.
Quane, S.L., Russell, J.K., 2005. Welding: insights from high-temperature analogue experiments. J. Volcanol. Geotherm. Res. 142 (1–2), 67–87.
Quane, S.L., Russell, K.J., Friedlander, E.A., 2009. Time scales of compaction in volcanic systems. Geology 37 (5), 471–474.
Ragan, D.M., Sheridan, M.F., 1972. Compaction of Bishop Tuff, California. GSA Bull. 83, 95–106.
Reedman, A.J., Park, K.H., Merriman, R.J., Kim, S.E., 1987. Welded tuff infilling a volcanic vent at Weolseong, Republic of Korea. Bull. Volcanol. 49, 541–546.
Robert, G., Russell, J.K., Giordano, D., 2008. Rheology of porous volcanic materials: high-temperature experimentation under controlled water pressure. Chem. Geol. 256 (3), 216–230.
Ross, C.S., Smith, R.L., 1961. Ash-flow tuffs, their origin, geological relations and identification. U. S. Geol. Surv. Prof. Pap. 366.
Russell, J.K., Quane, S.L., 2005. Rheology of welding: inversion of field constraints. J. Volcanol. Geotherm. Res. 142 (1–2), 173–191.
Russell, J.K., Giordano, D., Dingwell, D.B., 2003. High-temperature limits on viscosity of non-Arrhenian silicate melts. Am. Mineral. 88, 1390–1394.
Santos, J.O.S., 1984. Classificação das rochas vulcânicas Uatumã. 33rd Congresso Brasileiro de Geologia, Rio de Janeiro, Brazil, Abstracts (in Portuguese).
Santos, J.O.S., 2003. Geotectônica dos Escudos da Guiana e Brasil Central. In: Bizzi, L.A., Schobbenhaus, C., Vidotti, R.M., Gonçalves, J.H. (Eds.), Geologia, tectônica e recorsos minerais do Brasil. Texto, mapas e SIG. CPRM — Serviço Geológico do Brasil, Brasilia, pp. 169–226.
Santos, J.O.S., Hartmann, L.A., Gaudette, H.E., Groves, D.I., McNaughton, N.J., Fletcher, I.R., 2000. A new understanding of the provinces of the Amazon Craton based on integration of field mapping and U–Pb and Sm–Nd geochronology. Gondwana Res. 3, 453–488.
Santos, J.O.S., Groves, D.I., Hartmann, L.A., Moura, M.A., McNaughton, N.J., 2001. Gold deposits of the Tapajós and Alta Floresta Domains, Tapajós–Parima orogenic belt, Amazon Craton, Brazil. Miner. Deposita 36, 279–299.
Santos, J.O.S., Van Breemen, O.B., Groves, D.I., Hartmann, L.A., Almeida, M.E., McNaughton, N.J., Fletcher, I.R., 2004. Timing and evolution of multiple Paleoproterozoic magmatic arcs in the Tapajós Domain, Amazon Craton: constraints from SHRIMP and TIMS zircon, baddeleyite and titanite U–Pb geochronology. Precambrian Res. 13, 73–109.
Schmincke, H.-U., Swanson, D.A., 1967. Laminar viscous flowage structures in ash-flow tuffs from Gran Canaria, Canary Islands. J. Geol. 75, 641–664.
Silva Simões, M.S., Almeida, M.E., de Souza, A.G.H., da Silva, B.D.P.B., Rocha, P.G., 2014. Characterization of the volcanic and hypabissal rocks of the Paleoproterozoic Iricoumé Group in the Pitinga region and Balbina Lake area, Amazonian Craton, Brazil: petrographic distinguishing features and emplacement conditions. J. Volcanol. Geotherm. Res. 286, 138–147.
Smith, R.L., 1960. Zones and zonal variations in welded ash flows. U. S. Geol. Surv. Prof. Pap. 354-F, 149–158.
Smith, T.R., Cole, J.W., 1997. Somers Ignimbrite formation: cretaceous high-grade ignimbrites from South Island, New Zealand. J. Volcanol. Geotherm. Res. 75, 39–57.
Sumner, J.M., Branney, M.J., 2002. The emplacement history of a remarkable heterogeneous, chemically zoned, rheomorphic and locally lava-like ignimbrite: 'TL' on Gran Canaria. J. Volcanol. Geotherm. Res. 115, 109–138.
Tassinari, C.C.G., Macambira, M.J.B., 1999. Geochronological provinces of the Amazonian craton. Episodes 22, 174–182.
Teixeira, W., Tassinari, C.C.G., Cordani, U.G., Kawashita, K., 1989. A review of the geochronology of the Amazonian craton: tectonic implications. Precambrian Res. 42, 213–227.
Vasquez, M.L., Dreher, A.M., 2011. Uma avaliação da estratigrafia dos eventos magmáticos de 1900–1860 Ma do Cráton Amazônico. SBG, Simpósio Geologia da Amazônia, 12, Bol. Res.
Vasquez, M.L., Sousa, C.S., Carvalho, J.M.A. (Orgs.), 2008. Mapa Geológico e de Recursos Minerais do Estado do Pará, escala 1:1.000.000. Programa Geologia do Brasil, Belém, CPRM.
Wadsworth, F.B., Vesseur, J., von Aulock, F.W., Scheu, B., Lavallée, Y., Hess, K.-U., Dingwell, D.B., 2014. Non-isothermal viscous sintering of volcanic ash. J. Geophys. Res. Solid Earth 119. http://dx.doi.org/10.1002/2014JB011453.
Walker, G.P.L., 1983. Ignimbrite types and ignimbrite problems. J. Volcanol. Geotherm. Res. 17, 65–88.
Walker, G.W., Swanson, D.A., 1968. Laminar flowage in a Pliocene soda rhyolite ash-flow, Lake and Harney Counties, Oregon. U. S. Geol. Surv. Prof. Pap. 600B, 37–47.
Wolff, J.A., Wright, J.V., 1981. Rheomorphism of welded tuffs. J. Volcanol. Geotherm. Res. 10, 13–34. http://dx.doi.org/10.1016/0377-0273(81)90052-4.